Microwave Zebra Pattern Structures in the X2.2 Solar Flare on Feb 15, 2011

Baolin Tan[1], Yihua Yan[1], Chengming Tan[1], Robert Sych[1,2], Guannan Gao[3,1]

[1]*Key Laboratory of Solar Activity, National Astronomical Observatories Chinese Academy of Sciences, Beijing 100012, China*

[2] *Institute of Solar-Terrestrial Physics of Siberian Branch of Russian Academy of Sciences 126a Lermontov Street, Irkutsk, 664033, Russia*

[3] *National Astronomical Observatories/Yunnan Astronomical Observatories Chinese Academy of Sciences, Kunming 650011, Yunnan Province, China*

ABSTRACT

Zebra pattern structure (ZP) is the most intriguing fine structure on the dynamic spectrograph of solar microwave burst. On 15 February 2011, there erupts an X2.2 flare event on the solar disk, it is the first X-class flare since the solar Schwabe cycle 24. It is interesting that there are several microwave ZPs observed by the Chinese Solar Broadband Radiospectrometer (SBRS/Huairou) at frequency of $6.40 \sim 7.00$ GHz (ZP1), $2.60 \sim 2.75$ GHz (ZP2), and the Yunnan Solar Broadband Radio Spectrometer (SBRS/Yunnan) at frequency of 1.04 – 1.13 GHz (ZP3). The most important phenomena is the unusual high-frequency ZP structure (ZP1, up to 7.00 GHz) occurred in the early rising phase of the flare, and there are two ZP structure (ZP2, ZP3) with relative low frequencies occurred in the decay phase of the flare. By scrutinizing the current prevalent theoretical models of ZP structure generations, and comparing their estimated magnetic field strengths in the corresponding source regions, we suggest that the double plasma resonance model should be the most possible one for explaining the formation of microwave ZPs, which may derive the magnetic field strengths as about 230 – 345 G, 126 – 147 G, and 23 – 26 G in the source regions of ZP1, ZP2, and ZP3, respectively.

Subject headings: Sun: flares — Sun: fine structure — Sun: microwave radiation

1. Introduction

After a super-long quietness, the Sun begins a new Schwabe cycle. On 15 February 2011, there erupts an X2.2 flare event in active region NOAA AR11158 on the solar disk, which was the first X-class GOES flare of the current solar Schwabe cycle 24. Several instruments observed this event, including Solar Dynamics Observatory (SDO), Nobeyama Radio Polarimeter (NoRP) and Nobeyama Radio Heliograph (NoRH), RHESSI, Chinese Solar Broadband Radio Spectrometer (SBRS/Huairou), and Yunnan Solar Broadband Radio Spectrometer (SBRS/Yunnan). Especially from the broadband radio spectrogram observations at SBRS/Huairou and SBRS/Yunnan, strong microwave bursts with spectral fine structures, such as zebra patterns (ZP) and some other fine structures are registered. The most interesting and important phenomena is the microwave ZP structures. We have registered three ZP structures at different frequency bands and in different phases of the flare. We will focus on investigating these ZP structures in this work.

[1]Datun Road A20, Chaoyang District, Beijing, 100012, China.

ZP is a fine spectral structure superposed on the solar radio broadband type IV continuum spectrogram, which consists of several almost parallel and equidistant stripes. Most often, ZP structures are observed in meter and decimeter frequency range(Slottje, 1972, etc). In microwave range such structure is very rare. From the publications heretofore, the highest frequency at which ZP structure has been observed is about 5.70 GHz (Altyntsev et al, 2005). Recently, Chernov et al (2011) find out some ZP evidences at frequency of $5.70 \sim 7.20$ GHz from the observations of a solar flare on May 29, 2003 obtained at SBRS/Huairou. However, it is far infrequent to observe ZP structure at such high frequency range. Additionally, ZP structures are typically occurred around the impulsive phase and/or decay phase of solar flares. It is very rare to find ZP structure in the early rising phase of solar flare.

The formation mechanism of ZP structures has been a subject of widely discussion for more than 40 years. The historical development of observations and theoretical models are assembled in the review of Chernov (2006), Zlotnik (2009), and so on. There are several theoretical models to interpret ZP structures, which are mainly developed to apply to meter and decimeter wavelengths (Rosenberg, 1972; Kuijpers, 1975; Zheleznyakov & Zlotnik, 1975; Chernov, 1976, 1990; LaBelle, et al, 2003; Kuznetsev, 2005; Ledenev, et al, 2006; Tan, 2010; etc). These models can be classified simply into three classes:

(1) Isogenous models, which proposed that all the stripes in a ZP structure are generated from a small compact source.

The model of Bernstein mode (BM model) is the first one to interpret the formation of ZP structure. The emission mechanism is the nonlinear coupling between two Bernstein modes, or Bernstein mode and other electrostatic upper hybrid waves. The electrons with non-equilibrium distribution over velocities perpendicular to the magnetic field are located in a small source, where the plasma is weakly magnetized ($f_{pe} \gg f_{ce}$), and the magnetic field is uniform. These electrons excite longitudinal electrostatic waves at frequency of the sum of so-called Bernstein modes frequency sf_{ce} and the upper hybrid frequency f_{uh}. The BM excitation occurs in relatively narrow frequency band. The emission frequency (Rosenberg, 1972; Chiuderi et al, 1973; Zaitsev and Stepanov, 1983) is:

$$f = f_{uh} + sf_{ce} \approx f_{pe} + sf_{ce}. \tag{1}$$

Here, f_{pe} is the electron plasma frequency, f_{ce} the electron gyro-frequency, s is harmonics number. This model presents the frequency separation between the adjacent zebra stripes just as the electron gyro-frequency: $\Delta f = f_{ce}$ (Zheleznyakov and Zlotnik, 1975).

(2) Heterogenous models, which proposed that zebra stripes in a structure are generated from some extended source regions in the magnetic flux tube (Kuijpers, 1975; Fomichev and Fainshtein, 1981; Mollwo, 1983; Ledenev, Yan, and Fu, 2001; Chernov et al, 2005; Altyntsev et al, 2005).

One of the important heterogenous model is based on the plasma waves interact with whistler waves (Chernov, 1996, 2006), called as whistler wave model (WW model). The coupling of plasma wave and whistler wave can operate in different conditions: when whistlers generate at the normal Doppler cyclotron resonance they can escape along the magnetic loop and yield fiber bursts; when whistlers generate at the anomalous Doppler cyclotron resonance under large angles to the magnetic field they may form standing wave packets in front of the shock wave, and when the group velocity of whistlers is approximated to the shock velocity, a ZP structure with slow oscillating frequency drift will appear. The whistler wave group velocity peaks at whistler frequency $f_w \sim 0.25 f_{ce}$. The frequency separation Δf between adjacent zebra stripes is about 2 times of whistler frequency: $\Delta f \sim 2f_w$, and then we may obtain: $f_{ce} \sim 2\Delta f$.

The most developed heterogenous model for ZP structure generation is called double plasma resonance model (DPR model), which explain ZP structure in a natural way (Pearlstein, et al, 1966; Zheleznyakov & Zlotnik, 1975; Berney & Benz, 1978; Winglee & Dulk, 1986; Zlotnik et al, 2003; Yasnov & Karlicky, 2004; Kuznetsov & Tsap, 2007). This model proposed that enhanced excitation of plasma waves occurs at some resonance levels where the upper hybrid frequency coincides with the harmonics of electron gyro-frequency in the inhomogeneous flux tube:

$$f_{uh} = (f_{pe}^2 + f_{ce}^2)^{1/2} = sf_{ce} \tag{2}$$

The emission frequency is dominated not only by the electron gyro-frequency, but also by plasma frequency. When the emission generates from the coalescence of two excited plasma waves, the polarization may be very weak, the emission frequency is $f \approx 2f_{pe} \approx 2sf_{ce}$, and the frequency separation between the adjacent zebra stripes is $\Delta f = \frac{2sf_{ce}H_b}{|sH_b-(s+1)H_p|}$. Here, $H_b = f_B(df_B/dr)^{-1} = B(dB/dr)^{-1}$ and $H_p = f_{pe}(df_{pe}/dr)^{-1} = 2n_e(dn_e/dr)^{-1} = 2H_n$. H_b and H_n are the scale heights of magnetic field B and the plasma density n_e in the source regions, respectively. For $f_{ce} \ll f_{pe}$ and $s \gg 1$, we may get:

$$\Delta f \approx \frac{2H_b}{|H_b - 2H_n|} f_{ce} \tag{3}$$

When the emission generates from coalescence of an excited plasma wave and a low frequency electrostatic wave, the polarization will be strong, the emission frequency is $f \approx f_{pe} \approx sf_{ce}$, and the frequency separation between the adjacent zebra stripes is $\Delta f = \frac{sf_{ce}H_b}{|sH_b-(s+1)H_p|}$. For $f_{ce} \ll f_{pe}$ and $s \gg 1$, we may get:

$$\Delta f \approx \frac{H_b}{|H_b - 2H_n|} f_{ce} \tag{4}$$

Equ. (3) and (4) indicate that the frequency separation between the adjacent zebra stripes is dominated by both the scale heights of the magnetic field and plasma density.

Ledenev et al (2001) proposed another heterogenous model to interpret the formation of ZP structures. This model (named as Ledenev model) suggests that the emission generated from an anisotropic energetic electron beam at low cyclotron harmonics in a significantly inhomogeneous magnetic field. The electron beam is formed as a result of fast local energy release in corona, such as magnetic reconnection, it will excite longitudinal waves at the normal Doppler resonance. The coalescence of upper-hybrid waves and low-frequency longitudinal waves ($U + L \rightarrow T$) can produce electromagnetic waves (T). This model gives the cyclotron frequency harmonics ratio as (Sawant et al, 2002):

$$\frac{f_s}{f_{s+1}} = \frac{f_{pe,s}}{f_{pe,s+1}} [\frac{s^3(s+2)}{(s+1)^3(s-1)}]^{1/2} \tag{5}$$

$f_{pe,s}$ and $f_{pe,s+1}$ are the electron plasma frequencies corresponding to the level of s and $s+1$ harmonics. If density changes slowly in source regions, then $f_{pe,s} \approx f_{pe,s+1}$, and the frequency ratio of the cyclotron frequency harmonics can be presented roughly as: $s = 2$, $f_2/f_3 \approx 1.089$; $s = 3$, $f_3/f_4 \approx 1.027$; $s = 4$, $f_4/f_5 \approx 1.012$; $s = 5$, $f_5/f_6 \approx 1.006$, etc. In this regime, the magnetic field strength in source region can be estimated: $B \approx \frac{f_{max}}{2.8\times10^6 s}, (G)$, here f_{max} is the frequency on the zebra stripe with maximum harmonic number s.

(3) Propagating model, which proposed that ZP stripes are formed in the propagating processes after emitted from its source region. The interference model which suggests that ZP is possibly formed from some interference mechanism in the propagating processes (Ledenev, Yan, and Fu, 2006). They suppose that there may exist some inhomogeneous layers with small size in solar coronal plasma, and such structure will change the radio wave into direct and reflected rays. When the direct and reflected rays meet at some places, interference will take place and form ZP structure. However, this model needs a structure with great number of discrete narrow-band sources in small size. Tan (2010) proposed that such structure may exist in the current-carrying flaring plasma loop, where the tearing-mode instability forms a great number of magnetic islands which may provide the main conditions for the interference mechanism.

ZP is the most intriguing fine structure on the dynamic spectrogram of solar radio observations, especially the microwave ZP structures, which may provide the original information of the solar flaring region, such as the magnetic field, particle acceleration, and the plasma parameters, etc. In this work, the observations and data analysis of the microwave ZP structures associated with the X2.2 flare are presented in Section 2, Section 3 is the physical discussion on the microwave ZP structures, especially the estimations of the magnetic field strengths from different ZP models, and pinpoint the reasonable interpretation of the ZP structures. At the final, some conclusions are summarized in Section 4.

2. Observations and Data Analysis

The active region AR11158 appeared near the center of the solar disk in the rising phase of the current solar cycle 24. It developed from a simple β- to a complex $\beta\gamma\delta$-configuration rapidly during 12 –21 February 2011. It produced an X2.2 flare on 15 February 2011. This flare was a two-ribbon white-light flare showed in the image of HMI/SDO, and accompanied with a large coronal mass ejection which launched just towards the Earth. From the soft X-ray emission obtained by GOES, the flare starts at 01:46 UT, reaches to the maximum at 01:56 UT, and ends at 02:07 UT (Maurya, Reddy, & Ambastha, 2011).

In this work, we focused on the observations obtained from SBRS/Huairou and SBRS/Yunnan. SBRS/Huairou is an advanced solar radio telescope with super high cadence, broad frequency bandwidth, and high frequency resolution, which can distinguish the super fine structures from the spectrogram (Fu et al 1995; Fu et al 2004; Yan et al, 2002). It includes 3 parts: 1.10 $\sim$ 2.06 GHz (with the antenna diameter of 7.0 m, cadence of 5 ms, frequency resolution of 4 MHz), 2.60 $\sim$ 3.80 GHz (with the antenna diameter of 3.2 m, cadence of 8 ms, frequency resolution of 10 MHz), and 5.20 $\sim$ 7.60 GHz (share the same antenna of the second part, cadence of 5 ms, frequency resolution of 20 MHz). The antenna points to the solar center of automatically controlled by a computer. The spectrometer can receive the total flux density of solar radio emission with dual circular polarization (left- and right handed circular polarization), and the dynamic range is 10 dB above quiet solar background emission. And the observation sensitivity is: $S/S_{\odot} \leq 2\%$, here $S_{\odot}$ is quiet solar background emission. Similar to other several spectrometers, such as Phoenix (100 $\sim$ 4000 MHz, Benz et al, 1991), Ondŕejov (800 $\sim$ 4500 MHz, Jiricka et al, 1993) and BBS (200 $\sim$ 2500 MHz, Sawant et al, 2001), SBRS/Huairou have no spatial resolution. However, as the Sun is a strong radio emission source, a great deal of works (e.g. Dulk, 1985, etc) show that the microwave bursts received by spectrometers are always coming from the solar active region when the antenna points to the Sun. Additionally, we also adopt the observations at SBRS/Yunnan, which operating frequency band is in 0.65 $\sim$ 1.50 GHz, with a spectral resolution of 1.4 MHz, and time resolution of 80 ms, by using a 10-meter diameter antenna.

During the X2.2 flare, SBRS/Huairou has two parts (2.60 $\sim$ 3.80 GHz and 5.20 $\sim$ 7.60 GHz) on

duty, SBRS/Yunnan and NoRP also obtained perfect radio observations. Fig.1 presents the profiles of the microwave flux at frequencies of 1.00, 2.00, 2.85, 3.75, 6.82, 9.40, 17.00, and 35.00 GHz in 01:45 $\sim$ 02:30 UT observed at SBRS/Huairou and NoRP. As a comparison, the profiles of GOES soft X-ray intensities at wavelengths of 1 $\sim$ 8 Å(GOES8) and 0.5 $\sim$ 4 Å(GOES4) are plotted in panel (9) of Fig.1. Additionally, the plasma temperature derived from the ratio of GOES soft X-ray emission fluxes at the two wavelength bands (Thomas, Starr, & Crannell, 1985) is also over-plotted. Here, we find that the maximum temperature (at about 01:53 UT) is prior to the GOES flare peak (01:56 UT) for about 3 minutes.

From the scrutinizing of the microwave spectrogram, we find that there is a strong microwave type IV burst with spectral continuum in the frequency range of 0.65 – 1.50, 2.60 – 3.80, 5.20 – 7.60 GHz, and the corresponding microwave enhancements are also occurred at frequency of 9.40, 17.00, 35.00 GHz. Superposed on these continuum enhancements, we identify many kinds of fine structures, such as type III bursts, spike bursts, patches, fast quasi-periodic pulsations (QPP), fibers and ZP structures. The main part of the microwave bursts at low frequencies occurred after the GOES flare peak. However, at the higher frequency range, the main part of the microwave bursts are prior to that of lower frequencies. Most of the fine structures are occurred at the moderate frequency band of 2.60 – 3.80 GHz after the GOES flare peak, only one segment of microwave ZP structure occurred prior to the GOES flare peak (marked as ZP1 in Fig.1) which frequency is around 6.70 GHz.

In this work, our interesting is mainly focused on microwave ZP structures. There are 3 segments of microwave ZP structures registered on the microwave spectrogram: the first one occurred at frequency of about 6.70 GHz (ZP1), the second one is at about 2.68 GHz (ZP2), and the third one is at about 1.08 GHz (ZP3). With a simple glance, we find that the higher frequency of ZP structure appears at the earlier flare phase, while the lower frequency of ZP structures take place in the later flare phase. The following is the details.

(1) Microwave ZP Structure at 6.40 $\sim$ 7.00 GHz

In the frequency of 5.20 $\sim$ 7.60 GHz, the microwave emission always behaves as continuous type IV burst, and the fine structure is very rare during solar flares. However, the most interesting phenomenon is an ZP structure occurred at frequency of around 6.70 GHz in the X2.2 flare. The left panel of Fig.2 is the spectrogram of the ZP structure observed at SBRS/Huairou. It shows that the frequency range of the structure is occurred from 6.40 to 7.00 GHz with a central frequency of 6.70 GHz. The time interval is from 01:49:50.2 to 01:49:51.5 UT, just at about 4 minutes after the onset of the flare (01:46 UT), and about 6 minutes before the GOES flare peak (01:56 UT). The duration of the ZP structure lasts for about 1.3 s. It is composed with 3 stripes in distorted sinusoidal wave shape arrayed on the longitudinal direction. The whole sinusoidal wave shape drifts slowly to the low frequency, and the drifting rate is about -300 MHz/s. The frequency bandwidth of the zebra stripes is about 40 $\sim$ 60 MHz. The frequency separation between the adjacent zebra stripes is about 80 $\sim$ 120 MHz, and the relative frequency separation is $\Delta f/f \simeq 1.17$ – 1.76 %, increases slowly with respect to time. The emission of the structure is strongly left-handed circular polarization with polarization degree (defined as $pol = \frac{R-L}{R+L} \times 100\%$, here R and L are the emission flux subtracted the background emission) close to 100%. Additionally, the ZP presents superfine structures: each zebra stripe consists of millisecond spikes which are practically vertical bright lines in the spectrogram with duration at the limit of the time resolution (5 ms) and the bandwidth of about 40 – 60 MHz.

The right panel of Fig. 2 is the temporal profile of the microwave flux at frequency of 6.80 GHz associated with the ZP1 structure. In this figure, the averaged level of the ambient background emission before and after the ZP structure is also presented (the dashed line) which is about 535 sfu at left- and right-handed

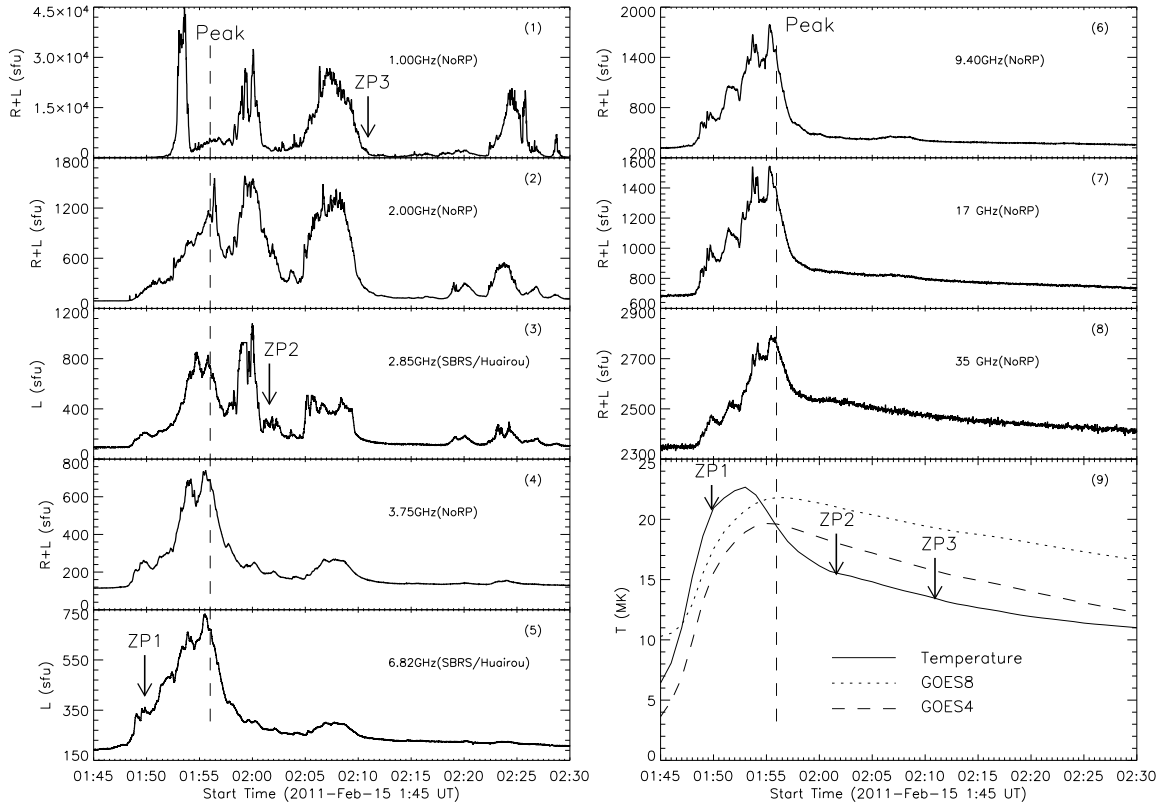

Fig. 1.— Panel (1) – (8) are profiles of the microwave flux at frequencies of 1.00, 2.00, 2.85, 3.75, 6.82, 9.40, 17, and 35 GHz in 01:45 $\sim$ 02:30 UT, 15 Feb. 2011. NoRP indicates the observation of Nobeyama Radio Polarimeter, and SBRS/Huairou indicates the observation of the Chinese Solar Broadband Radio Spectrometer (SBRS/Huairou). Panel (9) shows the GOES soft X-ray profiles at 1 $\sim$ 8 Å(GOES8) and 0.5 $\sim$ 4 Å(GOES4), and the plasma temperature induced from the GOES soft X-ray emission. The arrows indicate the positions of ZP structures on the profiles.

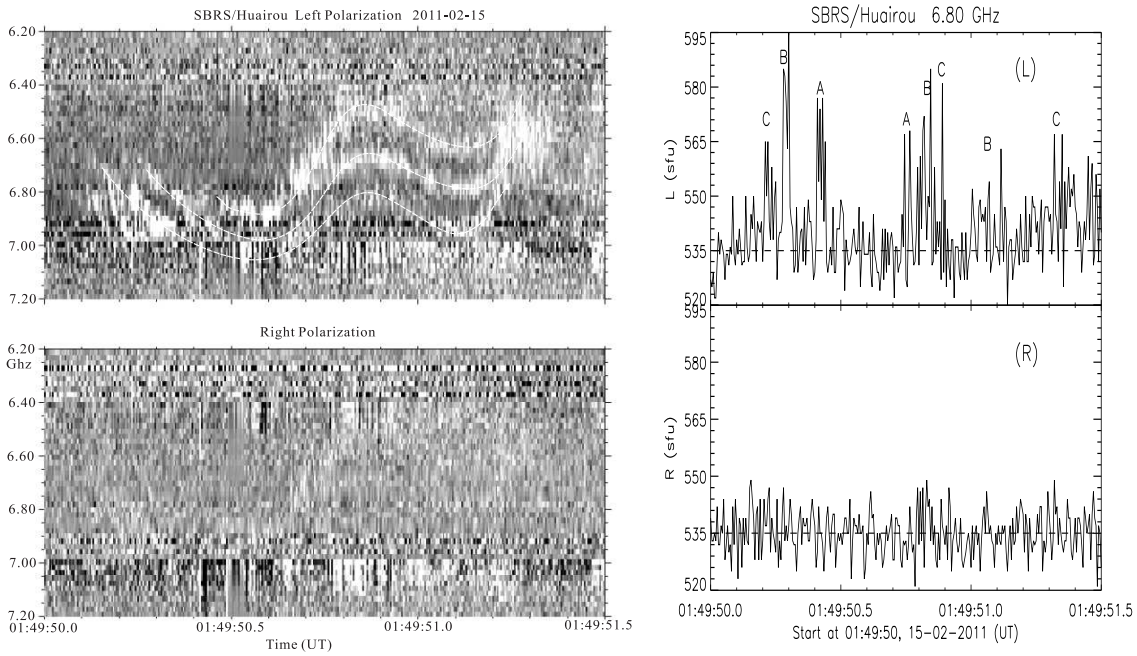

Fig. 2.— The left panel is the spectrogram of the Zebra pattern occurred at frequency of 6.40 ∼ 7.00 GHz observed at Chinese Solar Broadband Radiospectrometer (SBRS/Huairou) in 01:49:50 ∼ 01:49:51.5 UT, 15 Feb. 2011, the white dashed curves outshine the zebra stripes. The right panel is the profile of emission flux at frequency of 6.80 GHz in the same time interval of the Zebra pattern. A, B, and C represent respectively the stripes at high, middle, and low frequencies, which intersect with the horizontal level at frequency of 6.80 GHz in the left panel.

circular polarization. The intensity of the zebra stripes have enhancements of about $40 \sim 80$ sfu with respect to the ambient emissions, which is much higher than the instrument sensitivity (here $2\%S_{\odot}$ is about $4 \sim 5$ sfu at frequency of $6.20 \sim 7.20$ GHz). The positions of stripes are marked with letters (A, B and C, which represent respectively the stripes at high, middle, and low frequencies). At the same time, Fig. 2 is also implying another feature: the emission intensity on the zebra stripes decreases from the low frequency stripe to the high frequency stripes.

Fig.2 indicates that the zebra stripes of ZP1 are in distorted sinusoidal wave shapes. If we suppose that the pattern is a mixture of a general ZP structure and a quasi-periodic pulsation (QPP), then it is easy to understand the distorted sinusoidal wave shapes. Fig. 3 is the result of Fast Fourier Transformation (FFT) analysis on the microwave emission at frequency of 6.80 GHz, which indicates that the period of QPP is about 375 ms. This QPP belongs to a very short-period pulsation (VSP).

(2) Zebra Pattern Structure at $2.60 \sim 2.75$ GHz

The second ZP structure is a weakly one (marked as ZP2 in Fig. 1) at frequency of $2.60 \sim 2.75$ GHz in $02{:}01{:}19 \sim 02{:}01{:}21$ UT on the left-handed circular polarization spectrogram observed at SBRS/Huairou (Fig. 4). There are 2 stripes in this structure which can be discriminated from the spectrogram. The frequency separation between the adjacent zebra stripes is 60 – 70 MHz, and the relative frequency separation is about $\Delta f/f_0 \simeq 2.23$ – 2.60 %. The ZP structure lasts for about 1.5 s. It is very weak, that the emission flux at the zebra stripes is only $15 \sim 25$ sfu higher than that of the background emissions. In the first half part of the ZP structure, the frequency drift rate is about $26 \sim 42$ MHz/s, with averaged value is about 35 MHz/s. And in the second half part, the frequency drift rate reverses to about -67 $\sim$ -90 MHz/s, with averaged value about -78 MHz/s. The averaged value of the drift rate in the whole structure is approximated to 0. From Fig. 4, it is reasonable to assume that the ZP structure would be extended to the frequency range lower than 2.60 GHz and the stripe number should be > 2. However, as lack of observation at the lower frequency range, we couldn't confirm this conjecture.

From the background of ZP2 on the spectrogram, a fast quasi-periodic pulsation is also registered with frequency band of 2.62 – 2.90 GHz, and the period of about 30 ms. On the high frequency side of the ZP structure, there is a group of dot bursts occurred at 2.92 – 3.09 GHz, which frequency bandwidth is about 75 – 85 MHz, and the polarization degree is $pol \sim 30$ – 35 % at right-handed circular polarization, and the lifetime of single dot burst is in the range of 0.12 – 0.28 s. The distribution of the dots has a frequency drift rate of 180 MHz/s.

There are several clusters of fiber bursts on the spectrogram occurred after the flare peak at frequency of $2.60 \sim 3.00$ GHz. One example of fiber burst occurred in $02{:}03{:}34 \sim 02{:}03{:}43$ UT observed at SBRS/Huairou. The frequency drift rates of the fibers are in the range of -211.9 MHz/s $\sim$ -403.2 MHz, with averaged value of -303.5 MHz/s. This frequency drift rate is much faster than the previous observations (e.g., the value was in the range of 42.3 – 87.4 MHz/s in the observations at the similar frequency range of Wang & Zhong, 2006, etc.). The central frequency is about 2.80 GHz. The polarization of the fiber emission is strong left-handed circular polarized, and the polarization degree is $pol \sim$90%.

Two type III bursts is also observed at SBRS/Huairou. The first type III burst occurred at frequency of $2.62 \sim 2.90$ GHz in $02{:}07{:}50.70 \sim 02{:}07{:}50.85$ UT, the frequency bandwidth is 280 MHz, its frequency drift rate is in range of $11.25 \sim 11.67$ GHz/s. The emission is weakly right-handed circular polarization with $pol \simeq 15 \sim 20\%$. The second type III burst occurred at frequency of $2.64 \sim 2.93$ GHz in $02{:}07{:}51.55 \sim 02{:}07{:}51.67$ UT, the frequency bandwidth is 290 MHz, its frequency drift rate is around 12.81 GHz/s, and it is also weakly right-handed circular polarization with $pol \simeq$ 20-25%.

(3) Zebra Pattern Structure at 1.04 $\sim$ 1.13 GHz

There is an obvious ZP structure occurred at 1.04 $\sim$ 1.13 GHz in 02:10:56.8 $\sim$ 02:11:00 UT on 15 Feb. 2011, which is 15 minutes after the flare peak time, observed by SBRS/Yunnan, marked as ZP3 in Fig.1. Fig.6 presents the spectrogram, which indicates that there are 5 stripes in the ZP structure, and the duration is about 3.2 s. In the first half part of the structure (before 02:10:58.6 UT), the frequency drift rate approximates to 0, but in the second half part of the structure (after 02:10:58.6 UT) the frequency drift rate is about -98 MHz/s. The frequency separation between the adjacent zebra stripes is 14 $\sim$ 16 MHz, and the relative frequency separation of the zebra stripes is about $\Delta f/f \simeq 1.3$ %. The emission of the ZP structure is mildly right-handed circular polarization, with polarization degree $pol \sim 35 - 40\%$.

Recently, a similar ZP structure was registered at frequency of 1.20 – 1.40 GHz from the observations of the Frequency-Agile Solar Radio-telescope Subsystem Testbed (FST) and the Owens Valley Solar Array (OVSA) in the decay phase of an X1.5 flare on 14 December 2006 (Chen et al, 2011). The main properties (central frequency, frequency separation, and the frequency drifting rate, etc.) are very similar with ZP3 of this work.

Fig.6 presents the features of the image of extreme ultraviolet 171 Å observed at SDO/AIA and the solar radio intensity contours of the left (dashed) and right (solid) handed polarizations at frequency of 17 GHz observed at NoRH just one and a half minutes before ZP1, and only two minutes after the onset of the flare. From this figure, we find that flare eruptive process started from several separated small regions which behave as several small discrete bright points on the image at extreme ultraviolet 171 Å observed at SDO/AIA. And the microwave emission with maximum intensity at 17 GHz also distributed close to the small discrete bright points. These facts indicate that the magnetic reconnection and the energy release may break out from several places with small size. ZP1 just times at this rising phase, where most of the stored magnetic energy has not released, and the magnetic field in the active region keeps in strong status. The plasma in the magnetic loops may become very dense because of the confinement of strong magnetic field. The magnetic reconnection accelerates electrons to form anisotropic energetic electron beams, this electron beam can excite low frequency electrostatic waves, then couple with the upper-hybrid plasma waves, and forms the ZP structures.

Additionally, from Fig.1 we may find that the temperature associated with the source region plasma is about 22 MK, 16 MK, and 15 MK corresponding to the ZP structures occurred at frequency of 6.40 – 7.00 GHz, 2.60 – 2.75 GHz, and 1.04 – 1.13 GHz, respectively.

Table 1 is the brief summary of the ZP structures observed in this flare events. Here, the method of derived plasma density will be introduced in next section. We find that the frequency separation between zebra stripes increases with respect to the central emission frequency, and the number of zebra stripes decreases with respect to the central emission frequency.

In an ordinary ZP structure, the frequency separation between the adjacent stripes grows with the emission frequency: from 4 $\sim$ 5 MHz at 200 MHz to about 80 MHz at 3.0 GHz, and to about 150 $\sim$ 200 MHz at 5.70 GHz, and the relative frequency separation of stripes is about a constant: $\Delta f/f \simeq 2 \sim 3.5$ %. However, in this X2.2 flare event, we find that ZP1 and ZP3 has a narrow relative frequency separation of the zebra stripes, which is smaller than 1.8%, although the relative frequency separation of ZP2 stripes is very close to the above general ZP structure.

Table 2 presents the frequency ratio of the adjacent zebra stripes in each ZP structure. We find that the frequency ratios of the adjacent zebra stripes are approximated to a constant of about 1.020 in ZP1, and

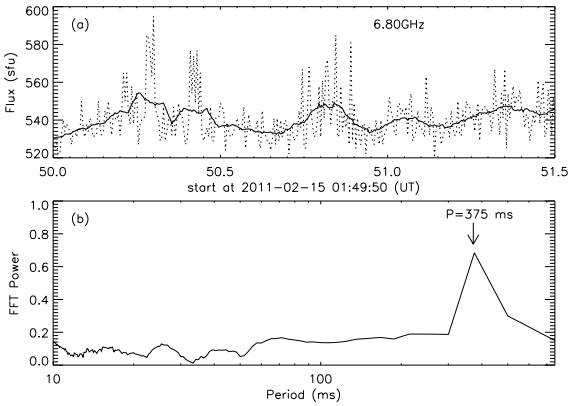

Fig. 3.— The FFT analysis on the microwave emission at frequency of 6.80 GHz, the upper panel is the profile of emission intensity, and the lower panel is the spectral power of the FFT analysis.

Table 1: Main features of the ZP structures associated with the X2.2 flare. f_0 is the central frequency, DR is the frequency drift rate, pol is the polarization degree, Δf is frequency separation of the zebra stripes, $\frac{\Delta f}{f_0}$ is the relative frequency separation of the zebra stripes, T is the temperature induced from the GOES soft X-ray emission.

ZP event	ZP1	ZP2	ZP3
Start (UT)	01:49:50.2	02:01:19.0	02:10:56.8
Duration (s)	1.3	1.5	3.2
Frequency Range (GHz)	6.40 – 7.00	2.60 – 2.75	1.04 – 1.13
f_0 (GHz)	6.70	2.68	1.08
DR (MHz/s)	-300	$+35 \sim$ -78	$0 \sim$ -98
pol (%)	90 – 100	90 – 100	35– 40
Δf (MHz)	80∼120	60∼70	14∼16
$\frac{\Delta f}{f_0}$(%)	1.17 – 1.76	2.23 – 2.60	1.30 – 1.48
stripes	3	>2	6
plasma density (cm^{-3})	5.5×10^{11}	8.8×10^{10}	1.4×10^{10}
T (MK)	22	16	15

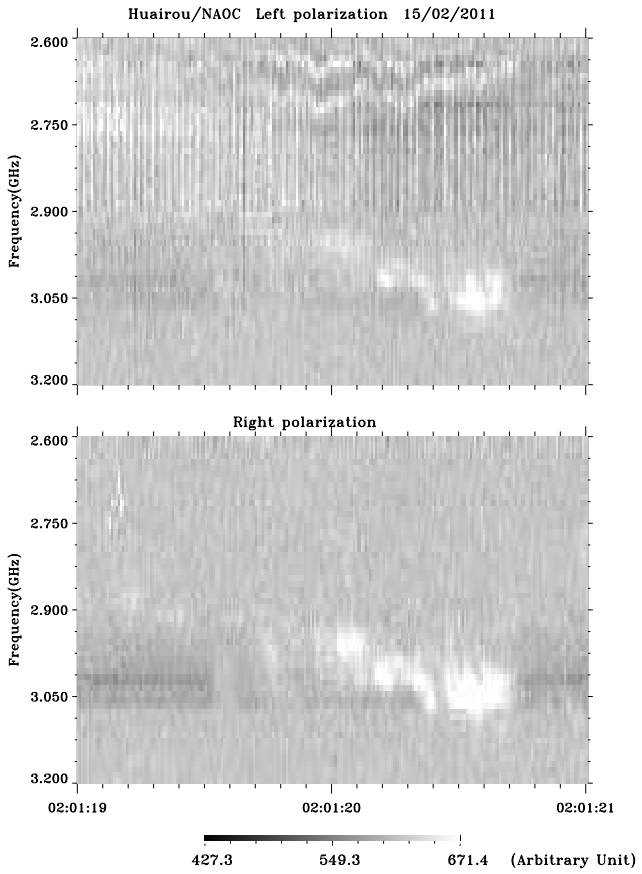

Fig. 4.— The spectrogram of a zebra pattern structure at frequency of 2.60 ∼ 2.75 GHz observed at Chinese Solar Broadband Radiospectrometer (SBRS/Huairou) in 02:01:19 ∼ 02:01:21 UT, on 15 Feb. 2011.

Table 2: Lists of the frequency, frequency ratio of the adjacent zebra stripes in each ZP structure.

ZP event	Stripe No.	Frequency(GHz)	Frequency Ratio
ZP1	1	6.80	
	2	6.66	1.021
	3	6.54	1.018
ZP2	1	2.73	
	2	2.65	1.030
ZP3	1	1.124	
	2	1.107	1.015
	3	1.094	1.012
	4	1.080	1.013
	5	1.066	1.013

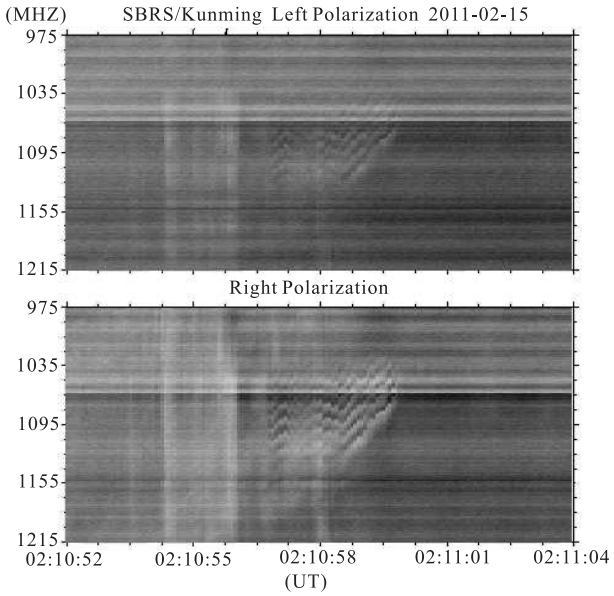

Fig. 5.— The spectrogram of a zebra pattern structure in the frequency of 1.04 ∼ 1.13 GHz observed by the Solar Broadband Radiospectrometer at Yunnan (SBRS/Yunnan) in 02:10:56.8 ∼ 02:11:00 UT, on 15 Feb. 2011.

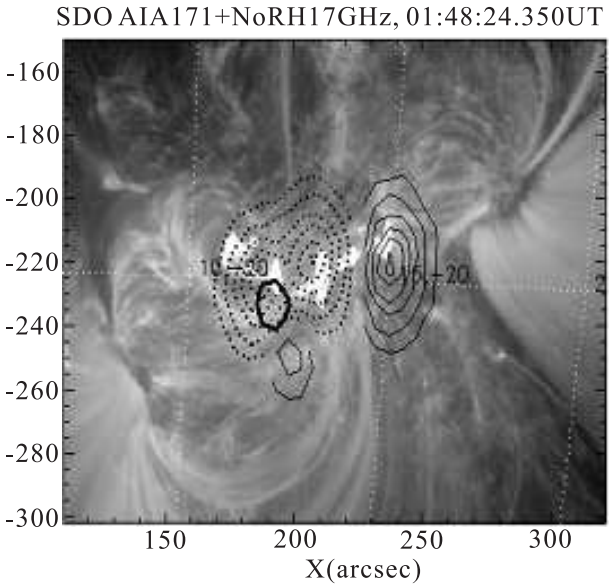

Fig. 6.— The solar microwave intensity contours of the left (dashed) and right (solid) handed polarizations at frequency of 17 GHz observed by NoRH overlapped on the background image of extreme ultraviolet 171 Å observed by SDO/AIA.

1.013 in ZP3. This feature is much more obvious in ZP3 where there are 5 zebra stripes, the maximum ratio is 1.015 while the minimum ratio is 1.012, all of them are very close to 1.013. This fact indicates that the Ledenev's model is not suitable to interpret the formation of the ZP structures observed in this work.

3. Physical Discussion on the Zebra Patterns

At first, almost all the theoretical models (BM model, WW model, or DPR model) for the generation of ZP structures indicate that the ZP emission frequencies are approximately around the plasma frequency or its second harmonics. With this point, the plasma density in the ZP source regions can be estimated: $n_e \approx f^2/81s^2$. As ZP1 and ZP2 have strongly polarization, $s = 1$. As for ZP3, its has moderate polarization degree (35 – 40%). According to the calculation of Dulk (1985), the polarization degree of the second harmonic plasma emission is only 10 – 20%. So, ZP3 also possibly belongs to the fundamental emission $s = 1$. Substituting the emission frequencies of ZP structures into this expression, the range of plasma density in the ZP source regions can be obtained, respectively:

ZP1, 5.1×10^{11} – 6.0×10^{11} cm^{-3}, the averaged value is 5.5×10^{11} cm^{-3};

ZP2, 8.3×10^{10} – 9.3×10^{10} cm^{-3}, the averaged value is 8.8×10^{10} cm^{-3};

ZP3, 3.3×10^{9} - 4.0×10^{9} cm^{-3}, the averaged value is 1.4×10^{10} cm^{-3}.

Generally, the source region with plasma density as up to 5.5×10^{11} cm^{-3} is always located very close to the base of solar corona where the height from the solar photosphere is only several thousands kilometers, while the source region with plasma density of about $\times 10^{10}$ cm^{-3} is located near the bottom of the solar corona. However, it should be different around the active regions, especially around the flaring regions. The X-ray observations indicate that the plasma densities around the flaring core region are in the range of $10^9 - 10^{11}$ cm^{-3}, and their heights can be in several decades of thousands km above the solar photosphere (Ohyama & Shibata, 1998).

One of the crucial and most difficult problem in solar physics is to determine the coronal magnetic field confidently. There are many publications which present the estimations of the coronal magnetic field by using solar radio observations (Mann, Karlicky, & Motschmann, 1987; Gelfreikh, 1998; Huang & Nakajima, 2002; Huang 2008, etc.). Recent observations of microwave bursts with fine structures open up a new possibilities for determining the coronal magnetic field (Karlicky & Jiricka, 1995; Lenedev et al, 2001, etc). The ZP structure is one of most important microwave fine structures which can be used to diagnose magnetic field strength in the coronal source regions, although the results depend on the theoretical models. Different ZP model will deduce different values of magnetic field in the ZP source region. Practically, it is always difficult to verdict which model is the best one fitted to observations. Possibly, from the estimations of the magnetic field strengths from the ZP structures, we could get a considerable restriction for the theoretical models.

(1) BM model indicates that the frequency separation of the adjacent zebra stripes is just equal to the electron gyro-frequency. From this we may obtain a direct measurement of the magnetic field in the coronal source region:

$$B \simeq \frac{2\pi m_e}{e}\Delta f \simeq 35.6 \times 10^{-8}\Delta f. \tag{6}$$

Here, the unit of B is in Gauss, and f in Hz. Substituting the frequency separation of ZP1, ZP2, and

ZP3 into the above expression, we may get the magnetic field strength as 28 – 43 G, 21 – 25 G, and 5 – 6 G, respectively. In this regime, the magnetic field strength is only depending on the frequency separation between the adjacent zebra stripes.

(2) From WW model, we may get the magnetic field strength in ZP source region:

$$B \simeq 2\frac{2\pi m_e}{e}\Delta f \simeq 71.2 \times 10^{-8}\Delta f \tag{7}$$

With this relation, the magnetic field strength is two times of that estimated from BM model: 55 – 85 G, 42 – 49 G, and 10 – 11 G, corresponding to ZP1, ZP2, and ZP3, respectively. This regime is also independent to the inhomogeneous scale height in the source region.

(3) From DPR model, we may obtain the measurement of magnetic field strength in the ZP structure source region. Based on Equation (3) and (4), the magnetic field strength can be derived:

$$B \simeq \frac{2\pi m_e}{e} \cdot Q \cdot \Delta f. \tag{8}$$

Here, Q is an inhomogeneous factor which is dominated mainly by the scale heights of plasma density n_e and the magnetic field B in the source region. It can be expressed as:

$$Q = \frac{|2H_n - H_b|}{sH_b}. \tag{9}$$

Here s is the harmonic number. When the emission generated from the coalescence of an excited plasma wave and a low frequency electrostatic wave, the emission frequency equals nearly to plasma frequency, $s = 1$ (fundamental emission); and when the emission generated from the coalescence of two excited plasma waves, the emission frequency equals nearly to the double plasma frequency, $s = 2$ (second harmonics).

The scale heights of plasma density H_n and the magnetic field H_b are two crucial parameters which control the magnitude of Q. However, they are depending on the atmospheric models around the source region. We may adopt the Newkirk model to express the plasma density around the source region: $n(r) = M \times 10^{\frac{4.32}{r}}$. M is a constant in the Newkirk model which may change depending on the different coronal regions. However, it does't change the following estimations when we change the magnitude of M (it doesn't appear in the expression of H_n). The scale height of plasma density can be deduced:

$$H_n \simeq 70r^2, (Mm). \tag{10}$$

As for the coronal magnetic field above active region, the Dulk & McLean model is always adopted: $B(r) = 0.5m/(r-1)^{1.5}, (1.02 \leq r \leq 10)$ (Dulk & McLean, 1978). However, this model represents only an averaged decrease of the magnetic field strength with height, the real values may deviate by a factor m of up to 3. r is the height from the solar center in unit of the solar optical radius $R_\odot$.

More precisely, we may take the coronal loop model to obtain the scale height of the magnetic field in ZP source regions, the magnetic field strength in a coronal loop can be written as: $B(h) \sim B_0(1 + h/d)^{-3}$ (Takakura, 1972). Here, B_0 is the magnetic field at the foot-point of the loop, d is the distance between the two foot-points, and h is the height from the photosphere. Then the scale height of magnetic field can be deduced as:

$$H_b = \frac{d}{3}(1 + \frac{h}{d}). \tag{11}$$

According to the work of Maurya, Reddy, & Ambastha (2011), we know that the maximum magnetic field on the sunspot is about 1400 G. From this figure, we also find that the distance between the maximum centers of left- and right-handed polarizations at frequency of 17 GHz is only about 40 arc-seconds, approximated to 29 Mm. Because the maximum centers of left- and right-handed polarizations at frequency of 17 GHz are close to the foot-points of the plasma loop, we may assume $d \sim 29$ Mm.

Equ (8) – (11) indicate that the magnetic field strength depends on another unbeknown key parameter: r or h, here, $h = (r-1)R_\odot$. As lack of the imaging observation at the corresponding frequencies, we may give some assumptions. Considering the frequency of ZP1 (6.40 – 7.00 GHz) and the previous works (review of Gary & Keller, 2004), its source region is very close to the core region of the flaring energy release, we may assume its height is about 20 Mm (above the solar photosphere). Then the heights of ZP2 and ZP3 can be deduced as 39 Mm and 61 Mm by Newkirk model and plasma emission mechanism. With above estimations, assumptions and observations, we may obtain the magnetic fields in the source regions of ZP1, ZP2 and ZP3 are 230 – 345 G, 126 – 147 G and 23 – 26 G, respectively. The values of ZP1 and ZP2 are very close to that estimated from Takakura model, and also close to that estimated from Dulk & McLean model when the factor $m = 3$. However, the value of ZP3 is only approaching to that estimated from Dulk & McLean model when the factor $m = 1$, much smaller than that estimated from Takakura model.

Additionally, there are several clusters of fiber bursts at frequency of 2.60 – 3.00 GHz which is very close to the frequency band of ZP2. The fiber bursts have been thought to be another promising way to diagnose the coronal magnetic field in the source region. It can be generated by packets of low frequency whistler waves propagating along the magnetic field lines of coronal loop. From the frequency drift rate, we can derive the magnetic field (Benz & Mann, 1998):

$$B \simeq \frac{\pi H_n m_e}{ec\sqrt{x} \cdot cos\theta} \frac{df}{dt} \approx 5.93 \times 10^{-20} \frac{H_n}{\sqrt{x} cos\theta} \frac{df}{dt}, (Tesla) \tag{12}$$

H_n can be calculated from Equ.(10) in about 78 Mm. $x = \frac{f_w}{f_{ce}}$ is the ratio between whistler frequency and the electron gyro-frequency, θ is the declining with respect to the magnetic field line. Generally, $\theta \sim 0$, and $x \sim 0.01$, then we may substitute the frequency drift rates of the fiber burst at frequency of 2.60 – 3.00 GHz, the magnetic field strength can be obtained as 98.6 – 187.7 G, with the averaged value of 143.1 G. This value covers the result estimated by DPR model of ZP2. It can be regarded as a collateral evidence for the estimations of magnetic field in the ZP source regions from DPR model.

Table 3 presents the magnetic field strengths obtained from different models in ZP source regions. As a comparison, we also listed the estimations from Dulk & McLean model (m = 1, 2, and 3) and Takakura model at the corresponding heights, respectively. We find that BM model and WW model present very low estimations of the magnetic field in ZP source regions; Dulk & McLean model gives a low estimations for ZP1 and ZP2 when m=1 or 2. The result of DPR model gets the furthest consistency with the Takakura model and the Dulk & McLean model with m=3 when estimate the magnetic fields in source regions of ZP1 and ZP2. Especially in ZP2, estimations of the magnetic field from DPR model and Takakura model are also consistent with the result obtained from fiber bursts at the similar frequency range. So, we prefer to suppose that the DPR model is possibly the real model for the ZP structures observed in this work. However, there is a 2 times difference between DPR model and Takakura model in ZP3 source region. It may just reflect

that the Takakura model is valid only within a magnetic loop. In our above estimations, the height of the ZP3 source region is about 61 Mm, which is more than two times of distance ($d \sim 29$ Mm) between the two foot-points of the loop, such height should be much higher than the loop-top. It is possible that the source region of ZP3 is located at another different magnetic loop with a larger d and a much low B_0. As lack of such observations, we can not confirm such inference.

In section 2 we have pointed out that ZP1 is possibly a mixture of a general ZP structure and a QPP, and the QPP is a very short-period pulsation (VSP). From the work of Tan, et al (2007) and Tan, et al (2010), we may suppose that the QPP is possibly a result of modulations of the resistive tearing-mode oscillations in the current-carrying flare plasma loops with high temperature. The panel (9) of Fig.1 indicates that temperature around ZP1 22 MK) is very close to the maximum of the profile, it is possible that the modulations of the resistive tearing-mode oscillations take place. The current-carrying plasma loop can drive the tearing-mode oscillation and modulate the microwave emission to form VSP. On this VSP background, some mechanism generate the ZP structure.

4. Conclusions

On 15 February 2011, there erupts an X2.2 flare event on the solar disk, which was the first X-class flare occurred since the solar cycle 24. Associated with this flare event, three microwave ZP structures at different frequencies are registered in different phases of the flare: the first is registered from SBRS/Huairou at frequency of $6.40 \sim 7.00$ GHz, which is very unusual at such high frequency band and in the early rising phase of the flare; the second is also registered from SBRS/Huairou, at frequency of 2.60 – 2.73 GHz in the decay phase of the flare, possibly it may extend to the frequency lower than 2.60 GHz; the third is registered from SBRS/Yunnan at frequency of 1.04 – 1.13 GHz, in the decay phase after far from the flare peak.

By scrutinizing the current prevalent theoretical models of ZP structures (including Bernstein model, whistler wave model, DPR model, and the Ledenev model), comparing their estimated magnetic field strengths in the corresponding source regions, we find that the DPR model is much more possible for explaining the generation of microwave ZP structures. It derived the magnetic field strengths as about 230 – 345 G, 126 – 147 G, and 23 – 26 G in the source regions of ZP1, ZP2, and ZP3, respectively. Comparison with the diagnostics of fiber bursts and the previous empirical model, we suggest that such estimations are acceptable.

It should be noted that DPR model is not self-contained when we adopt it to diagnose the magnetic

Table 3: Magnetic field strengths (unit in Gauss) estimated from different models in ZP source regions.

ZP event		ZP1	ZP2	ZP3
ZP BM model		28 – 43	21 – 25	5 – 6
ZP WW model		55 – 85	42 – 49	10 – 11
ZP DPR model		230 – 345	126 – 147	23 – 26
Dulk & McLean model:	m=1	102	38	19
	m=2	204	76	38
	m=3	306	114	57
Takakura model		290	109	48

fields in ZP source regions. It needs the supplement of the inhomogeneity model of plasma density and magnetic field. However, it is not easy to get the exact inhomogeneity models. So far, all the existing models (e.g. Dulk & McLean model, Takakura model, etc) of plasma density and magnetic field are proposed that the plasma density and magnetic field change with the height, and expressed as functions of height (r or h). Such method implies that the inhomogeneous scale heights of magnetic field is also a function of magnetic field, and this is the origin of the self-contradictions. We need a more perfect model which can provide the inhomogeneous scale lengths of plasma density and magnetic field, and they are independent of the magnitude of magnetic field strength. The magnetic field diagnostics of BM model and WW model are independent of the inhomogeneity models, they seem to be the perfect models to diagnose the magnetic field in the source region by ZP structures. But they are not likely to agree with the ZP structures observed in this work.

However, we should be noted that either the Dulk & McLean model, or the Takakura's model is only a simplified model. The actual regime during the microwave burst with ZP structures should be extremely dynamic processes, the real magnetic topology is also much more complex and changeable than the depiction of the above models. So far, the only thing we can do is to obtain the approximated estimations. The relative large difference of the magnetic estimations in ZP3 source region between DPR model and the Takakura's model just reflect that its source region should be located at different magnetic loop with different distance of the foot-points and different different initial magnetic field.

From the above discussions, we know that the exact inhomogeneity models of magnetic field and plasma density are most important. However, so far, because of lack of imaging observation with spatial resolutions in the corresponding frequencies, it is difficult to obtain the configuration features of the coronal magnetic field in the source region. To overcome such problems, we need some new telescopes, for example, the constructing Chinese Spectral Radioheliograph (CSRH, 0.4 - 15 GHz, will be finished before 2014) in the decimetric to centimeter-wave range (Yan et al, 2009) and the proposed American Frequency Agile Solar Radiotelescope (FASR, 50 MHz - 20 GHz) (Bastian, 2003). When these instruments begin to work, we may obtain the solar radio observations with high spatial-temporal resolutions at multi-frequency channels. One of the most important way to measure the coronal magnetic field is to probe ZP structures in each subareas with high spatial resolutions, and deduce the magnetic field from certain theoretical models. With these development, we will get more perfect understanding of the elementary processes in solar flares.

The authors would like to thank the anonymous referee for the helpful and valuable comments on this paper. We would also thank the the GOES, NoRP, NoRH, SDO/AIA, and SBRS/Huairou teams for providing observation data. This work is mainly supported by NSFC Grant No. 10733020, 10873021, 10921303, MOST Grant No. 2011CB811401, the National Major Scientific Equipment R&D Project ZDYZ2009-3, RFBR 10-02-00153 and 11-02-10000-k. This research was also supported by a Marie Curie International Research Staff Exchange Scheme Fellowship within the 7th European Community Framework Programme. The research carried out by Sych Robert at National Astronomical Observatories (NAOC) was supported by the Chinese Academy of Sciences Visiting Professorship for Senior International Scientists, grant No. 2010T2J24. Guannan Gao's work is supported by CAS-NSFC Key Project(Grant No.10978006).

REFERENCES

Altyntsev A. T., Kuznetsov A. A., Meshalkina N.S., Rudenko G. V., & Yan Y., 2005, *A&A*, **431**, 1037

Bastian T., 2003, *Proc. SPIE.*, **4583**, 98.

Benz A.O., Gudel, M., Isliker, H., Miszkowicz S. & Stehling W., 1991, *Solar Phys.*, **133**, 385.

Benz A. O., & Mann G., 1998, *A&A*, **333**, 1034

Berney M., & Benz A.O., 1978, *A&A*, **65**, 369

Chen B., Bastian T.S., Gary D.E., & Ju J, 2011, *ApJ*, **736**, 64

Chernov G.P., 1976, *Sov. Astron.*, **20**, 582

Chernov G.P., 1990, *Solar Phys.*, **130**, 75

Chernov G.P., 1996, *Astron Rep.*, **40**, 561

Chernov G.P., Yan Y.H., Fu Q.J., & Tan C.M., 2005, *A&A*, **437**, 1047

Chernov G.P., 2006, *Space Sci. Rev.*, **127**, 195

Chernov G.P., Sych R.A., Meshalkina N.S., & Tan C.M., 2011, *A&A*, submited

Chiuderi C., Giaghetti R., & Rosenberg H., 1973, *Solar Phys.*, **33**, 335

Dulk G.A. & McLEAN D.J., 1978, *Solar Phys.*, **57**, 279

Dulk G. A., 1985, *Ann. Rev. Astron. Astrophys.*, **23**, 169

Fomichev V. V., & Fainshtein S. M., 1981, *Solar Phys.*, **71**, 1071

Fu Q.J., Qin Z.H., Ji H.R., & et al, 1995, *Solar Phys.*, **160**, 97

Fu Q.J., Ji H.R., Qin Z.H. et al., 2004, *Sol. Phys.*, **222**, 167

Gary D.E., & Keller C.U., 2004, *Astrophys. Space Sci. Lib.*, **314**, Kluwer Academic Publishers

Gelfreikh G.B., 1998, *Astron. Soc. Pac. Conf. Ser.*, **155**, 110

Huang G.L., & Nakajima H., 2002, *New Astron.*, **7**, 135

Huang G.L., 2008, *Adv. Space Rew.*, **41**, 1191

Jiricka K., Karlicky M., Kepka O., & Tlamicha, A., 1993, *Solar Phys.*, **147**, 203.

Karlicky M., & Jiricka K., 1995, *Solar Phys.*, **160**, 121.

Kuijpers J., 1975, *A&A*, **40**, 405

Kuznetsov A.A., 2005, *A&A*, **438**, 341

Kuznetsov A.A., & Tsap Yu, 2007, *Solar Phys.*, **241**, 127

LaBelle J., Treumann R. A., Yoon P.H., & Karlichy, 2003, *ApJ*, **593**, 1195

Ledenev V. G., Yan Y, & Fu Q, 2001, *Chin. J. Astron. Astrophys.*, **1**, 475

Ledenev V. G., Karlicky M., Yan Y., & Fu Q., 2001, *Solar Phys.*, **202**, 71

Ledenev V. G., Yan Y., & Fu Q., 2006, *Solar Phys.*, **233**, 129

Mann G., Karlicky M., & Motschmann U., 1987, *Solar Phys.*, **110**, 381

Maurya R.A., Reddy V., & Ambastha A., 2011, *ApJ*, in press

Mollwo L., 1983, *Solar Phys.*, **83**, 305

Ohyama M., & Shibata K., 1998, *ApJ*, **499**, 934

Pearlstein L.D., Rosenbluth, M.N., & Chang, D.B., 1966, *Phys. Fluids*, **9**, 953

Rosenberg H., 1972, *Sol. Phys.*, **25**, 188

Sawant H.S., Subramanian K.R., Faria C., et al: 2001, *Solar Phys.*, **200**, 167.

Sawant H.S., Karlicky M., Fernandes F.C.R., & Cecatto J.R., 2002, *A&A*, **396**, 1015

Slottji C., 1972, *Sol. Phys.*, **25**, 210

Takakura T., 1972, *Sol. Phys.*, **26**, 151

Tan B.L., Yan Y.H., Tan Ch.M., & Liu Y.Y., 2007, *ApJ*, **671**, 964

Tan B.L., Zhang Y., Tan C.M., & et al, 2010, *ApJ*, **723**, 25

Tan B.L., 2010, *Astrophys. Space Sci.*, **325**, 251

Thomas R.J., Starr R., & Crannell C.J., 1985, *Solar Phys.*, **95**, 323

Wang S.J., & Zhong X.C., 2006, *Solar Phys.*, **236**, 155

Winglee R.M., & Dulk G.A., 1986, *ApJ*, **307**, 808

Yan Y.H., Tan C.M., Xu L., Ji H.R., Fu Q.J., & Song G.X., 2002, *Sci. Chin. A Suppl.*, **45**, 89.

Yan Y.H., Zhang J., Wang W., Liu F., Chen Z.J., & Ji G.S., 2009, *Earth. Moon. Planet*, **104**, 97.

Yasnov L., & Karlicky M.G., 2004, *Sol. Phys.*, **219**, 289

Zaitsev V. V. & Stepanov A. V., 1983, *Sol. Phys.*, **88**, 297

Zheleznyakov V.V., & Zlotnik E. YA, 1975, *Solar Phys.*, **44**, 461

Zlotnik E. Ya, Zaitsev V.V., Aurass H., Mann G., & Hofmann A., 2003, *A&A*, **410**, 1011

Zlotnik E. Ya, 2009, *Cent. Eur. Astrophys. Bull.*, **33**, 281